Isotope effects on turbulent transport and entropy transfer processes in toroidal plasmas

Motoki Nakata[1]†,

[1]National Institute for Fusion Science, Toki 509-5292, JAPAN

In this article, additional discussions on the nonlinear entropy transfer between turbulence and zonal flows are given for the isotope ion mass effects on the trapped-electron-mode (TEM) driven turbulent transport shown in Ref. 1. Spectral analyses with the triad entropy transfer function reveal that the case with heavier isotope ions indicates a relatively smaller negative transfer (from zonal flows to turbulence), which implies to the weaker nonlinear decay of zonal flows.

1. Introduction

Impact of isotope ion mass on the turbulent transport and plasma confinement is a long-standing issue for several decades in plasma and fusion research, despite the broad interests and the importance for realizing future burning plasmas. Many theoretical and numerical efforts, especially for ITG-driven turbulence [e.g., Ref. 2], have been devoted so far to resolve a discrepancy between the so-called gyro-Bohm scaling and the experimental observations indicating an improved confinement with the opposite ion mass dependence[3]. Recently, Nakata et al.[1] found that combined effects of the collisional TEM stabilization by the isotope ions and the associated increase in the impacts of the steady zonal flows at the near-marginal linear stability lead to the significant transport reduction with the opposite ion mass dependence in comparison to the conventional gyro-Bohm scaling. In this article, for participants of The 1st JPP Frontiers in Plasma Physics Conference, the ion mass impact on the nonlinear interactions between zonal flows and turbulence is further investigated by means of the entropy balance/transfer analyses.

Here, we briefly summarize the gyrokinetic simulation model used in GKV code[4], and the entropy balance/transfer diagnostics[5–7]. The electromagnetic gyrokinetic equation (in Fourier representation with $\boldsymbol{k}_\perp = k_x \nabla x + k_y \nabla y$) describing the time evolution of the perturbed gyrocenter distribution function $\delta f_{\rm s}^{\rm (g)}$ on the five-dimensional phase-space $(\boldsymbol{k}_\perp, z, v_\parallel, \mu)$ is given by

$$\left(\frac{\partial}{\partial t} + v_\parallel \boldsymbol{b}\cdot\nabla + i\omega_{\rm Ds} - \frac{\mu \boldsymbol{b}\cdot\nabla B}{m_{\rm s}}\frac{\partial}{\partial v_\parallel}\right)\delta g_{{\rm s}\boldsymbol{k}_\perp} - \frac{c}{B}\sum_{\Delta} \boldsymbol{b}\cdot(\boldsymbol{k}'_\perp \times \boldsymbol{k}''_\perp)\,\delta\psi_{{\rm s}\boldsymbol{k}'_\perp}\delta g_{{\rm s}\boldsymbol{k}''_\perp}$$
$$= \frac{e_{\rm s} F_{\rm Ms}}{T_{\rm s}}\left(\frac{\partial \delta\psi_{\boldsymbol{k}_\perp}}{\partial t} + i\omega_{*T{\rm s}}\delta\psi_{\boldsymbol{k}_\perp}\right) + C_{\rm s}(\delta g_{{\rm s}\boldsymbol{k}_\perp}) \ , \qquad (1.1)$$

where the subscript "s" is the index of particle species, and $\delta g_{{\rm s}\boldsymbol{k}_\perp}$ stands for the non-adiabatic part of the perturbed gyrocenter distribution function $\delta f^{\rm (g)}_{{\rm s}\boldsymbol{k}_\perp}$, i.e., $\delta g_{{\rm s}\boldsymbol{k}_\perp} = \delta f^{\rm (g)}_{{\rm s}\boldsymbol{k}_\perp} + e_{\rm s} J_{0{\rm s}} \delta\phi_{\boldsymbol{k}_\perp} F_{\rm Ms}/T_{\rm s}$. The gyro-averaged potential fluctuation is denoted by $\delta\psi_{\boldsymbol{k}_\perp} := J_{0{\rm s}}[\delta\phi_{\boldsymbol{k}_\perp} - (v_\parallel/c)\delta A_{\parallel \boldsymbol{k}_\perp}]$, where $J_{0{\rm s}} := J_0(k_\perp v_\perp/\Omega_{\rm s})$ is the zeroth-order Bessel function, and the former and latter terms mean the electrostatic and electromagnetic parts in low-β limit, respectively. The symbol $\sum_\Delta$ appearing in the nonlinear term of Eq. (1.1) means the double summations with respect to $\boldsymbol{k}'_\perp$ and $\boldsymbol{k}''_\perp$, which satisfy the triad-interaction condition of $\boldsymbol{k}_\perp = \boldsymbol{k}'_\perp + \boldsymbol{k}''_\perp$. Note that the notations follow the usual convention, e.g., the particle mass, the electric charge, the equilibrium temperature, and the gyrofrequency are denoted by $m_{\rm s}$, $e_{\rm s}$, $T_{\rm s}$, and $\Omega_{\rm s} = e_{\rm s}B/m_{\rm s}c$, respectively.

† Email address for correspondence: nakata.motoki@nifs.ac.jp

By using the gyrokinetic and the Poisson-Ampère equations, one can derive another important equation describing the balance and transfer of the entropy variable $\delta S_{s\boldsymbol{k}_\perp} := \langle \int d\boldsymbol{v}\, |\delta f_{\boldsymbol{k}_\perp}|^2/2F_{\mathrm{Ms}}\rangle_z$ defined with the particle (not gyrocenter here) distribution function $\delta f_{\boldsymbol{k}_\perp} = -e_{\mathrm{s}}\delta\phi_{\boldsymbol{k}_\perp}F_{\mathrm{Ms}}/T_{\mathrm{s}} + \delta g_{s\boldsymbol{k}_\perp} e^{-i\boldsymbol{k}_\perp\cdot\boldsymbol{\rho}_{\mathrm{s}}}$,

$$\sum_{\mathrm{s}}\left(\underbrace{\frac{d}{dt}T_{\mathrm{s}}\delta S_{\mathrm{s}}^{(\mathrm{trb})}}_{(\mathrm{i})}\underbrace{+T_{\mathrm{s}}\delta R_{\mathrm{s}}^{(\mathrm{trb})}}_{(\mathrm{ii})}\underbrace{+T_{\mathrm{s}}\mathcal{T}_{\mathrm{s}}}_{(\mathrm{iii})}\underbrace{-T_{\mathrm{s}}\Omega_{\mathrm{s}}^{(\mathrm{trb})}}_{(\mathrm{iv})}\underbrace{-T_{\mathrm{s}}D_{\mathrm{s}}^{(\mathrm{trb})}}_{(\mathrm{v})}\right) = 0\,, \tag{1.2}$$

$$\sum_{\mathrm{s}}\left(\underbrace{\frac{d}{dt}T_{\mathrm{s}}\delta S_{\mathrm{s}}^{(\mathrm{zf})}}_{(\mathrm{i})}\underbrace{+T_{\mathrm{s}}\delta R_{\mathrm{s}}^{(\mathrm{zf})}}_{(\mathrm{ii})}\underbrace{-T_{\mathrm{s}}\mathcal{T}_{\mathrm{s}}}_{(\mathrm{iii})}\underbrace{-T_{\mathrm{s}}D_{\mathrm{s}}^{(\mathrm{zf})}}_{(\mathrm{v})}\right) = 0\,, \tag{1.3}$$

where the superscripts "(trb)" and "(zf)" mean the non-zonal and zonal components in the wavenumber space, respectively, i.e., $X^{(\mathrm{trb})} := \sum_{k_x}\sum_{k_y\neq 0} X_{k_x,k_y}$, $X^{(\mathrm{zf})} := \sum_{k_x} X_{k_x,k_y=0}$. Each term represents (i) the variation of the entropy variable, (ii) the variation of the field energy due to the wave-particle interactions, (iii) the nonlinear entropy transfer from non-zonal to zonal modes, (iv) the entropy production by turbulent particle and heat fluxes, and (v) the collisional dissipation, respectively (see, e.g., Refs. 5 and 6 for their definitions). Note that, by the definition, the turbulent-flux driven entropy production term does not appear for the zonal modes in Eq. (1.3). The entropy balance/transfer equation provides us with a good measure for the turbulence simulation accuracy as well as useful physical insights associated with the turbulence saturation mechanisms. The detailed numerical analyses of the entropy balance and the transfer processes in ITG turbulence are shown in, e.g., Refs. 6 and 7.

The definition of the entropy transfer function $\mathcal{T}_{s\boldsymbol{k}_\perp}$ for arbitrary $\boldsymbol{k}_\perp$ is given by

$$\mathcal{T}_{s\boldsymbol{k}_\perp} = \sum_{\boldsymbol{p}_\perp}\sum_{\boldsymbol{q}_\perp}\delta_{\boldsymbol{k}_\perp+\boldsymbol{p}_\perp+\boldsymbol{q}_\perp,0}\,\mathcal{J}_{\mathrm{s}}\left[\boldsymbol{k}_\perp|\boldsymbol{p}_\perp,\boldsymbol{q}_\perp\right]\,, \tag{1.4}$$

$$\mathcal{J}_{\mathrm{s}}\left[\boldsymbol{k}_\perp|\boldsymbol{p}_\perp,\boldsymbol{q}_\perp\right] = \left\langle \frac{c}{B}\boldsymbol{b}\cdot(\boldsymbol{p}_\perp\times\boldsymbol{q}_\perp)\int d\boldsymbol{v}\,\frac{1}{2F_{\mathrm{Ms}}}\mathrm{Re}\left[\delta\psi_{\boldsymbol{p}_\perp}h_{s\boldsymbol{q}_\perp}h_{s\boldsymbol{k}_\perp} - \delta\psi_{\boldsymbol{q}_\perp}h_{s\boldsymbol{p}_\perp}h_{s\boldsymbol{k}_\perp}\right]\right\rangle, \tag{1.5}$$

where the notation with $\boldsymbol{k}'_\perp$ and $\boldsymbol{k}''_\perp$ shown in Eq. (1.1) is replaced by $-\boldsymbol{p}_\perp$ and $-\boldsymbol{q}_\perp$, respectively, in order to represent symmetrically the triad-interaction condition for three wavenumber vectors, i.e., $\boldsymbol{k}_\perp + \boldsymbol{p}_\perp + \boldsymbol{q}_\perp = 0$. We call the function $\mathcal{J}_{\mathrm{s}}[\boldsymbol{k}_\perp|\boldsymbol{p}_\perp,\boldsymbol{q}_\perp]$ the "triad (entropy) transfer function", hereafter. It should be noted that the triad transfer function possesses the following symmetry properties,

$$\mathcal{J}_{\mathrm{s}}\left[\boldsymbol{k}_\perp|\boldsymbol{p}_\perp,\boldsymbol{q}_\perp\right] = \mathcal{J}_{\mathrm{s}}\left[\boldsymbol{k}_\perp|\boldsymbol{q}_\perp,\boldsymbol{p}_\perp\right]\,, \tag{1.6}$$

$$\mathcal{J}_{\mathrm{s}}\left[\boldsymbol{k}_\perp|\boldsymbol{p}_\perp,\boldsymbol{q}_\perp\right] = \mathcal{J}_{\mathrm{s}}\left[-\boldsymbol{k}_\perp|-\boldsymbol{p}_\perp,-\boldsymbol{q}_\perp\right]\,. \tag{1.7}$$

Furthermore, one obtains straightforwardly the "detailed balance relation" for the triad-interactions,

$$\mathcal{J}_{\mathrm{s}}\left[\boldsymbol{k}_\perp|\boldsymbol{p}_\perp,\boldsymbol{q}_\perp\right] + \mathcal{J}_{\mathrm{s}}\left[\boldsymbol{p}_\perp|\boldsymbol{q}_\perp,\boldsymbol{k}_\perp\right] + \mathcal{J}_{\mathrm{s}}\left[\boldsymbol{q}_\perp|\boldsymbol{k}_\perp,\boldsymbol{p}_\perp\right] = 0\,. \tag{1.8}$$

The entropy transfer function integrated over the zonal modes, $\mathcal{T}_{\mathrm{s}}$, represents the transfer of the entropy fluctuation from turbulence to zonal flows so that the positive and negative signs of $\mathcal{T}_{\mathrm{s}}$ appear in Eqs. (1.2) and (1.3), respectively. Note that $\mathcal{T}_{\mathrm{s}}$ is regarded as a kinetic extension of the zonal-flow energy production due to the Reynolds stress. Actually, by using the simplest approximation for the non-adiabatic part of the ion gyrocenter distribution function, i.e., $\delta g_{i\boldsymbol{k}_\perp} \simeq n_0 F_{\mathrm{Mi}}(1 + k_\perp^2\rho_{\mathrm{ti}}^2/2)e\delta\phi_{\boldsymbol{k}_\perp}/T_{\mathrm{i}}$, one can reduce $\mathcal{T}_{\mathrm{i}}$ to the conventional hydrodynamic energy production, which is described by the product of the Reynolds stress and the zonal-flow shear.

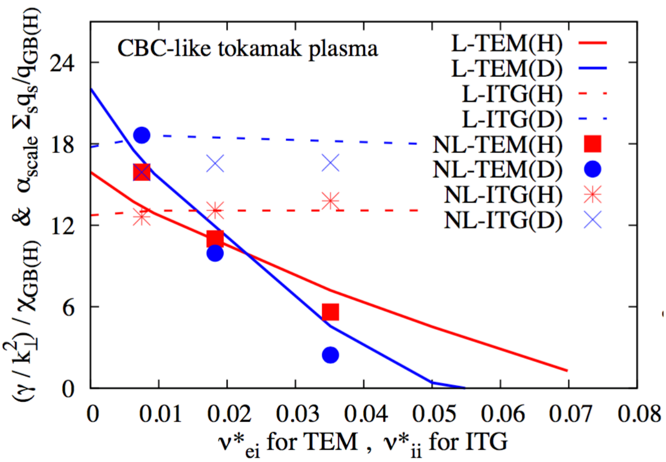

FIGURE 1. Collisionality dependence of the mixing-length diffusivity $\gamma/k_\perp^2$ for the linear TEM(solid lines) and ITG(dashed lines) modes in CBC-like tokamak H- and D-plasmas. Turbulent heat flux $\sum_s q_s$ obtained from nonlinear simulations are shown by symbols, where the values are uniformly scaled such that NL-TEM(H) and NL-ITG(H) match with L-TEM(H) and L-ITG(H) at $\nu^*_{ei} = 0.018$, respectively.

2. Turbulent transport reduction by isotope ion mass

Following Ref. 1, the reduction of the TEM-driven turbulent transport by the isotope ion mass effect is briefly demonstrated, where we examine the TEM (and ITG) turbulence in CBC-like tokamak plasmas with the equilibrium parameters of $\{R_{ax}/L_{T_i} = 1,\ R_{ax}/L_{T_e} = 8,\ R_{ax}/L_n = 3,\ T_e/T_i = 3\}$ for the TEM case and $\{R_{ax}/L_{T_i} = 8,\ R_{ax}/L_{T_e} = 8,\ R_{ax}/L_n = 3,\ T_e/T_i = 1\}$ for the ITG case. The so-called $s-\alpha$ toroidal geometry with $q(\rho_0) = 1.42$, $\hat{s}(\rho_0) = 0.8$, and $a\rho_0/R_{ax} = 0.18$ is considered.

The linear and nonlinear GKV simulation results for H- and D-plasmas are summarized in Fig. 1, where the collisionality dependencies of the mixing-length diffusivity $(\gamma/k_\perp^2)/\chi_{GB(H)}$ and turbulent heat flux $\sum_s q_s/q_{GB(H)}$ in the TEM and ITG cases are compared. Note that the hydrogen gyro-Bohm units, $\chi_{GB(H)}$ and $q_{GB(H)}$, are used for the normalization. For the cases in ITG modes (labeled by L-ITG in the figure) with weak ν^*_{ii} dependence, we see that the mixing-length diffusivity show a gyro-Bohm like mass dependence, i.e., $\gamma/k_\perp^2 \propto \sqrt{A_s}$. The similar $\sqrt{A_s}$ dependence is found in the collisionless limit of TEM (labeled by L-TEM in the figure). However, different reduction tendency of the TEM growth rates depending on the isotope ion species is revealed in the finite collisionality regime, where the ion mass dependence in the ratio of the electron-ion collision frequency to the ion transit one, i.e., $\nu_{ei}/\omega_{ti} \propto (m_i/m_e)^{1/2}$, leads to stronger collisional stabilization of TEM for heavier isotope ions. Note also that the stabilization effect on ITG modes by the ion-ion collisions is almost independent of the ion mass, i.e., $\nu_{ii}/\omega_{ti} \propto m_i^0$. Accordingly, the opposite ion mass dependence of $A_s^{-\alpha}$ with $\alpha > 0$ appears for TEM in a certain collisionality regime, i.e., $\nu^*_{ei} \geqslant 0.025$ in the present case.

It is also revealed that the turbulent heat fluxes in both the ITG and TEM driven turbulence (labeled by NL-ITG and NL-TEM) show the qualitatively similar dependence with the linear results, where the scaling constants of $\alpha_{scale} = 0.787\times10^{-2}$ and $\alpha_{scale} = 1.05\times10^{-2}$ are, respectively, multiplied to NL-ITG and NL-TEM values such that the nonlinear result in the H-plasma at $\nu^*_{ei} = 0.018$ matches the linear one for qualitative comparisons of the profile. We also see that, for larger ν^*_{ei}, the TEM driven turbulent transport obtained from the nonlinear simulation is smaller than the mixing length estimation. This tendency is because the turbulence suppression by zonal flows becomes stronger as the TEM growth rate decreases towards the marginal stability with increasing ν^*_{ei}. The strong impact of the TEM-driven zonal flow on the turbulence suppression is

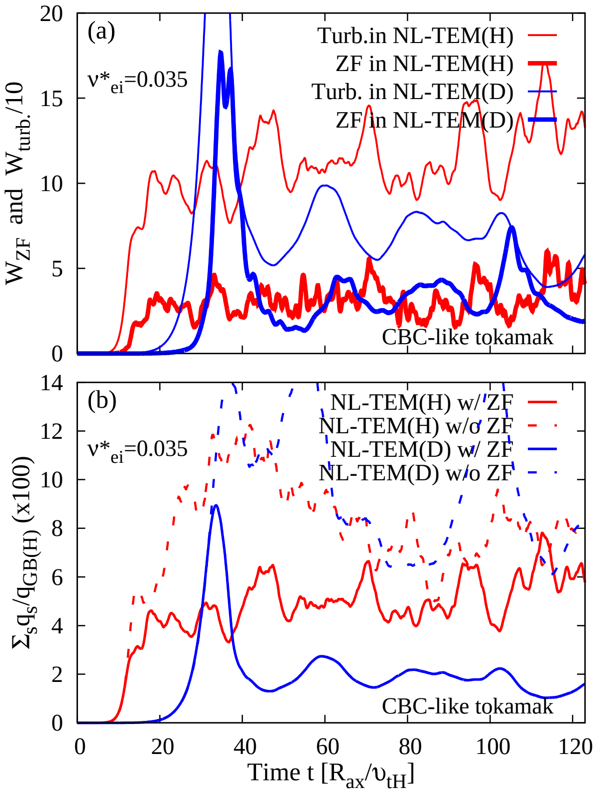

FIGURE 2. (a)time evolution of the zonal-flow (thick lines) and turbulence (thin lines) energy in tokamak TEM turbulence with hydrogen and deuterium ions, where $\nu_{\mathrm{ei}}^{*} = 0.035$. (b)the turbulent heat flux in the cases with (solid lines) and without (dashed lines) zonal-flow components.

also shown in Fig. 2(b), where the numerical simulations with and without the zonal components are compared. It has been clarified that, as shown in Fig. 2(a), the relative amplitude of the steady zonal flows, $\overline{W}_{\mathrm{ZF}}/\overline{W}_{\mathrm{turb.}}$, is enhanced in the near-marginal TEM case with $\nu_{\mathrm{ei}}^{*} = 0.035$ resulting from the collisional stabilization by heavier isotope ions, while the lower and comparable amplitudes are found in H- and D-plasmas with relatively higher TEM growth rates. Indeed, the absolute values of the zonal-flow energy W_{ZF} in D-plasmas are kept to be the similar level to that in H-plasma, despite the decrease of the turbulence energy which is the nonlinear source of the zonal-flow generation [Fig. 2(a)]. Note also that the effective zonal-flow shearing rate compared to the maximum growth rate, $\omega_{\mathrm{ZF}}/\gamma_{\mathrm{max}}$, in D-plasma is more than twice as large as those in H-plasma, where $\omega_{\mathrm{ZF}} = \langle|\partial_x v_{\mathrm{ZF}}|\rangle_x$, and $\langle\cdots\rangle_x$ means the spatial average in the x direction.

3. Entropy transfer for zonal modes

Underlying mechanisms of the zonal flow enhancement in the near-marginal stability for D-plasma are analyzed by using the entropy balance relation with the triad entropy transfer function given in Eq. (1.4). From gyrokinetic entropy balance equation for zonal modes, Eq. (1.3), with

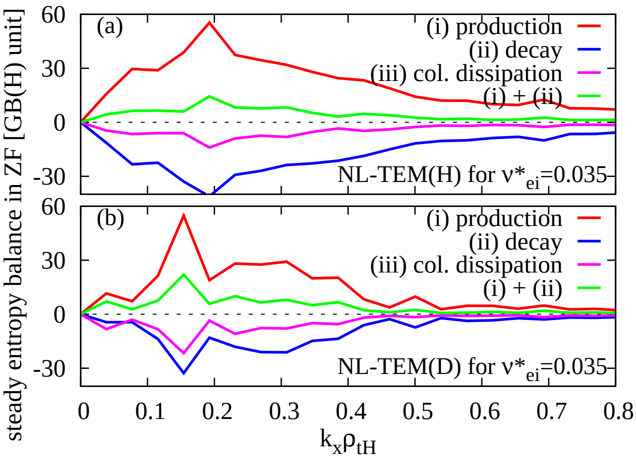

FIGURE 3. Radial wavenumber(k_{zf}) spectra of the nonlinear (i) production($\mathcal{T}^{(+)}_{sk_{zf}}$), (ii) decay($\mathcal{T}^{(-)}_{sk_{zf}}$), and (iii) collisional dissipation($\mathcal{D}^{(ZF)}_{sk_{zf}}$) for zonal flows in the tokamak (a)H- and (b)D-plasmas with $\nu^*_{ei} = 0.035$, corresponding to Fig. 1.

the radial wavenumber of k_{zf}, one can derive a balance relation in the steady turbulence state, i.e., $\sum_s T_s \mathcal{T}^{(+)}_{sk_{zf}} = -\sum_s T_s[\mathcal{T}^{(-)}_{sk_{zf}} + \mathcal{D}^{(ZF)}_{sk_{zf}}]$ (the overline symbol for long-time average is omitted). Here, the nonlinear production(+) and decay(-) are described by $\mathcal{T}^{(\pm)}_{sk_{zf}} = \sum_{\boldsymbol{q}_\perp}(1/2)[\mathcal{G}_{sk_{zf}}(\boldsymbol{q}_\perp) \pm |\mathcal{G}_{sk_{zf}}(\boldsymbol{q}_\perp)|]$, where $\mathcal{G}_{sk_{zf}}(\boldsymbol{q}_\perp) = \mathcal{J}_s[\boldsymbol{k}_{zf}\,|\,\boldsymbol{p}_\perp = -(\boldsymbol{k}_{zf} + \boldsymbol{q}_\perp),\ \boldsymbol{q}_\perp]$ denotes the triad entropy transfer function for zonal modes. Figures 3(a) and 3(b) show the comparison of k_{zf}-spectra in the nonlinear production($\mathcal{T}^{(+)}_{sk_{zf}}$), nonlinear decay($\mathcal{T}^{(-)}_{sk_{zf}}$), and collisional dissipation($\mathcal{D}^{(ZF)}_{sk_{zf}}$) terms for H- and D-plasmas with $\nu^*_{ei} = 0.035$ corresponding to Fig. 1. It is found that, for D-plasma at near-marginal stability, the relative magnitude of the nonlinear decay (due to e.g., tertiary instability of zonal modes[8–10]) characterized by $|\mathcal{T}^{(-)}_{sk_{zf}}|/|\mathcal{T}^{(+)}_{sk_{zf}}|$ is smaller than that for H-plasma with higher TEM growth rate. This is analogous to the steady entropy balance and transfer for the ITG-driven zonal flows in the Dimits-shift regime[7], but we need further deeper analyses of the isotope ion mass (and also magnetic geometry) impacts on the tertiary modes for zonal flows.

REFERENCES

[1] M. Nakata *et al.*, Phys. Rev. Lett. 118, 165002 (2017)
[2] A. Bustos *et al.*, Phys. Plasmas 22 012305 (2015)
[3] M. Bessenrodt-Weberpals *et al.*, Nucl. Fusion 33, 1205 (1993)
[4] T. -H. Watanabe *et al.*, Nucl. Fusion 46, 24 (2006)
[5] H. Sugama *et al.*, Phys. Plasmas 16, 112503 (2009)
[6] M. Nakata *et al.*, Phys. Plasmas 19, 022303 (2012)
[7] M. Nakata *et al.*, Nucl. Fusion 53, 113039 (2013)
[8] B. N. Rogers *et al.*, Phys. Rev. Lett. 85, 5336 (2000)
[9] G. G. Plunk *et al.*, New J. Phys. 14 103030 (2012)
[10] G. G. Plunk *et al.*, The 1st JPP Frontiers in Plasma Physics Conference (2017)